Carbonatite Melts and Electrical Conductivity in the Asthenosphere

Gaillard F[1], Malki M[2] , Iacono-Marziano G[1,3], Pichavant M[1], Scaillet B[1]

Corresponding author: *gaillard@cnrs-orleans.fr*

[1] CNRS/INSU, Université d'Orléans, Université François Rabelais - Tours,
Institut des Sciences de la Terre d'Orléans - UMR 6113
Campus Géosciences, 1A, rue de la Férollerie, 41071 Orléans cedex 2, France.

[2] CEMHTI-CNRS, UPR3079, 1D avenue de la Recherche Scientifique, 45071 Orléans cedex2, France.
[2] Polytech'Orléans – Université d'Orléans, 8 rue Léonard de Vinci, 45072 Orléans cedex 2, France.
[3] Istituto Nazionale di Geofisica e Vulcanologia, sezione di Palermo, Via Ugo La Malfa 153, 90146 Palermo, Italy.

Abstract:

Electrically conductive regions in the Earth mantle have been interpreted to reflect the presence of either silicate melt or water dissolved in olivine. On the basis of laboratory measurements we show that molten carbonates have electrical conductivities that are 3 orders of magnitude higher than those of molten silicate and 5 orders of magnitude higher than those of hydrated olivine. High conductivities in the asthenosphere probably indicate the presence of small amounts of carbonate melt in peridotite and can therefore be interpreted in terms of carbon concentration in the upper mantle. We show that the conductivity of the Oceanic asthenosphere can be explained by 0.1 volume % of carbonatite melts on average, which agrees with the CO_2 content of Mid Ocean Ridge Basalts.

Laboratory measurements on anhydrous peridotite and olivine single crystals indicate that the electrical conductivity of the upper mantle, if dry, should be ~ 10^{-4}-10^{-2} S.m^{-1} with the higher values reflecting high mantle temperatures *(1, 2)*. Deep magnetotelluric data however, indicate that the electrical conductivity of some mantle regions exceeds these values *(3, 4, 5)*. In the Pacific Ocean mantle, for example, conductivities of >10^{-1} S.m^{-1} have been measured at depth > 60 km *(4, 5)*. Such zones require the presence of conductive phases; silicate melts or hydrated olivine crystals are commonly considered *(3, 5, 6, 7, 8)*. Silicate melts have electrical conductivities of 10^{-2}-10^{1} S.m^{-1} *(6, 7, 9, 10)* but peridotite melting requires high temperatures or high water content *(11)*. The high mantle conductivities have therefore usually been interpreted as indicating trace amounts of hydrogen in olivine *(4, 5, 8, 12)*. Direct measurements in mantle xenoliths provide compelling evidence for hydrated mantle olivine *(13)*. However, the magnitude of the effect of water on olivine conductivity remains under debate *(14, 15)*. Furthermore, it is unclear how hydrated olivine can produce high electrical anisotropy measured in the asthenospheric mantle *(15)*. We present here experimental data showing that molten carbonates (i.e. carbonatites) can potentially explain high mantle conductivities.

The carbon dioxide content of mantle derived magmas is a few hundred ppmw in mid ocean ridge basalts and can reach a few thousand ppmw in specific settings *(16, 17)*, which constrains the CO_2 content of the mantle source to a few tens to hundreds ppmw *(16, 17, 18)*. Under most of the pressure-temperature-oxygen fugacity conditions prevailing in the upper mantle, carbon is likely to be present in the form of molten carbonates *(19-22)*. Such carbonatite melts have exceedingly large wetting properties *(23)*: they form interconnected liquid networks at olivine grain boundaries even at very low volume fractions *(23, 24)* and could therefore contribute to the electrical conductivity of the mantle. The available data on the electrical conductivity of molten carbonates cover Li-rich compositions of industrial interest *(25)*. However, mantle carbonatites are particularly Li-poor and Mg, Ca-rich, and have variable K and Na *(26)*. We measured the electrical conductivity of molten Li-free and Ca-rich carbonates. Our measurements were performed at 1 atmosphere of CO_2 pressure using a 4-electrode experimental method adapted to greatly conductive molten materials [*(27)* and

Supporting online material]. No magnesium carbonate was included in our material because Mg-bearing molten carbonates are not stable at 1 atm pressure. The high conductivities of carbonate melts shown below make challenging conductivity measurements with conventional setup at high pressure. Pressure effects are probably minor, as discussed below.

Our data show that the electrical conductivity of molten carbonate increases from 50 to 200 $S.m^{-1}$ as temperature increases from 400 to 1000°C (Fig. 1, S8; Table 1). Such conductivity values are comparable to those reported on Li-rich molten carbonates [*(25)*, SOM]. Molten carbonates at 1000°C are 1000 times as conductive as molten silicates *(6, 7, 9, 10)* at the same temperature and at least 100,000 times as conductive as hydrous and dry olivine single crystals *(2, 14, 15)*. In our measurements, the electrical conductivity of molten carbonates varied slightly with chemical composition. Calcium-free carbonates containing 30 mole % Li_2CO_3 were about 2 to 3 times as conductive as a Li-free melt containing 50 mole % $CaCO_3$ (Fig. 1, S8; Table 1). Another feature of molten carbonate conductivities is their small temperature dependence. The temperature dependence of molten carbonate electrical conductivities (σ) can be adequately fitted using an Arrhenius law:

$$\sigma = \sigma_0 \times \exp [-Ea / (RT)] \quad (1)$$

The derived pre-exponential terms (σ_0) and the activation energies (E_a) for each investigated composition are in Table 1. Activation energies are 30-35 kJ/mol, which is about one third of the average E_a for natural molten silicates [70-150 kJ/mol; *(6, 7, 9, 10)*] and one tenth of those for dry olivine [200-300 kJ/mol; *(2)*]. Such low activation energies are similar to those (38 kJ/mol) reported for the viscosity of synthetic molten carbonates of composition $(K_2Ca)(CO_3)_2$ *(28)*. Furthermore, we calculated (see Table S1) that the diffusing process responsible for the electrical conductivity and the viscosity of molten $(K_2Ca)(CO_3)_2$ are similar (~10^{-9} $m^2.s^{-1}$ at 1000°C). This suggests that, unlike silicate melts *(9, 10)*, both viscosity and electrical conductivity of carbonate melts entail similar transport mechanisms. Extrapolation to mantle conditions requires an evaluation of the effect of $MgCO_3$ on the conductivity of molten carbonates, as mantle carbonatites should contain 5-15 wt% MgO at equilibrium with mantle minerals *(26)*, and of the effect of pressure. In view of the

similarities between conductivity and viscosity, both effects can be deduced from the effect of $MgCO_3$ and pressure on the viscosity of molten carbonates. Magnesium-bearing molten carbonates are slightly less viscous than those Mg-free *(28)*. We therefore expect that the conductivities of Mg-bearing carbonatites are slightly higher than those of Mg-free molten carbonates. Experimental data *(28)* and molecular dynamics calculations *(29)* indicate that pressure has little effect on the viscosity of molten carbonates up to mantle pressures. We thus conclude that mantle carbonatites should preserve the high conductivity we determined at 1 bar (SOM). The electrical conductivity of mantle carbonatites can therefore reasonably be described by the Arrhenius equation given in Table 1.

Molten carbonates are therefore by far the most conductive phase of Earth's upper mantle. High electrical conductivity globally observed in the asthenosphere *(3)* could therefore reveal small amounts of carbonatite melts hosted in the mantle. As an example of application of these data, we focus on the asthenosphere below the Pacific Oceanic ridge. This region of the mantle has been relatively well studied by geophysical imaging *(4,5)*, and petrological evidence suggests that small quantities of carbonatite liquids are formed in such asthenospheric mantle at depths of up to ~300 km *(19,20)*. The geophysical surveys imaged a resistive body ($\sigma \sim 10^{-2}$-10^{-3} $S.m^{-1}$) consistent with anhydrous peridotite in the upper 60 km of the mantle *(4,5)*, which corresponds to the oceanic lithosphere. A conductive structure ($\sigma \sim 1$-10^{-1} $S.m^{-1}$) extends down to 200 km below the ridge axis *(5)*. A structure of nearly comparable conductivity ($\sigma \sim 10^{-1}$-10^{-2} $S.m^{-1}$) extends in the direction perpendicular to the ridge axis on the East-side of the ridge at depths between 70 and 120 km *(4,5)*. Such structure was not observed on the West-side of the axis *(4,5)*. Both conductive structures show strong anisotropy that cannot be account for by hydrated olivine crystals *(15)*. An additional conductive component is therefore needed and the presence of silicate melt has been suggested *(15)*.

Figure 2 shows in a conductivity-depth plot the different electrical structures of the Pacific Ocean mantle described above. We also show electrical conductivities calculated for different model mantles consisting of dry and hydrous olivine, dry olivine with 5-30 vol.% MOR-basalt and dry olivine with variable amounts of carbonatite melt. All calculated conductivities vary with depth following an

adiabatic path *(19,20)*. The deep conductive asthenosphere (70-200 km) underneath the ridge axis can be explained considering olivine mixed with between 0.035 to 0.35 vol.% of carbonatite. Olivine with more than 5 % of basalt could alternatively account for the high conductivity of this region but elevated degree of peridotite melting is precluded at such depth *(11, 19)*. Hydrous olivine is unable to account for such a high conductivity domain *(14, 15)*. The presence of small amount of carbonatite is therefore the best explanation for the high conductivity of this region. Furthermore, the range 0.035-0.35 vol. % of carbonatite corresponds *(30)* on average to ~300 ppmw CO_2 stored in the asthenosphere, in reasonable agreement with the variable estimates of CO_2 concentrations in the source region of MOR-basalts *(16-18, 31)*. The off-axis conductive asthenosphere (depths of 70-120 km in Fig.2) can not be explained by olivine with a few percent of basalt, because it extends at depths inconsistent with silicate melting *(11)*. Hydrous olivine may account for its lowermost conductivity, but not for the upper range of values. From our results, the off-axis asthenosphere can be interpreted as olivine with ~0.005-0.035 % of carbonatite melts.

It has been shown that the off-axis conductive zone joins the deep asthenosphere underneath the ridge *(5)*. Carbonatite melts underneath the ridge derive from the decompression melting initiating at depths of 300 km *(20)*, while their presence extending 350 km eastward of the ridge at depths of 70-120 km might result from their lateral migration. Based on conductivities shown in Fig. 2, we suggest that ~$1/10^{th}$ of the carbonatite melt produced in the asthenosphere underneath the ridge may flow laterally in the mantle. The rest would migrate upwards and be incorporated in the silicate melts deriving from peridotite melting at depths ~70-80 km below the ridge. The CO_2 contents in MORBs and their heterogeneity *(16-18)* would therefore originate from the incorporation of small amount of carbonatite melts by basaltic melts.

Figure captions:

Figure 1. Electrical conductivity versus temperature for the most important mantle phases (dry and hydrous olivine, molten silicates, and molten carbonates). SO3 refers to anhydrous olivine conductivity *(2)*. For hydrous olivine, we show experimental datasets of *(14, 15)*. The two curves labeled (Yo), which exhibit the lowest conductivity in the hydrous olivine field, are on oriented single olivine crystals containing 100-150 ppmw water *(15)*. Each curve corresponds to crystallographic axes yielding the fastest and the slowest conduction. The upper curve labeled (W) refers to olivine aggregates with 100 ppmw water dissolved in olivine *(14)*. For silicate melts, anhydrous results are shown in red and hydrous in blue. From the less to the more conductive, results for (a) a dry MOR-basalt at 2 GPa *(7)*, (b) a dry MOR-basalt at 1 bar *(7)*, (c) a dry alkali basalt at 1 bar *(6,10)*, (d) a hydrous silica-rich melt at 1 bar *(9)* and (e) an hydrous alkali basalts at 1 bar *(10)* are shown. In the upper part of the diagram, the conductivities of molten carbonates are presented, extrapolated from our experiments at 400-1000°C using eq. 1 (see Fig. S8). From the less to the more conductive, we show $(KCa_{0.5})_2(CO_3)_2$, $(NaKCa_{0.5})_2(CO_3)_3$, $(NaKCa)(CO_3)_2$, $(NaK)_2(CO_3)_2$, and $(LiNaK)_2(CO_3)_3$.

Figure 2. Electrical conductivity (and resistivity in brackets) versus depth calculated assuming adiabatic temperature changes *(19)* (i.e. $T_{300\ km}$ ~1420°C) for dry olivine (grey line), hydrous olivine (blue line), dry olivine with 5 and 30 vol.% of basalt (green lines), and dry olivine with 0.005, 0.035, 0.35 vol.% of carbonatite melt (red lines). For the calculation of electrical conductivity of mixtures, we assume a Hashin-Shtrikman upper bound that implies an interconnected melt between olivine grains *(6)*. Dry olivine conductivity is calculated from *(2)* and the hydrous olivine is calculated after *(15)* for crystals containing ~150 ppmw water (average between fast and slow crystallographic orientation). The olivine + 5% basalt is calculated by taking the conductivity of dry basalt at 1 bar *(7)*; increasing pressure would decrease the conductivity of such a mixture but the magnitude of the pressure effect differs between different laboratory studies *(7, 9, 10)*. The olivine – carbonatite mixtures are calculated after the conductivity of mantle carbonatite given in Table 1. The asthenosphere conductivity below the Pacific ridge [*(5)*, red box] is best explained by olivine with 0.035-0.35% of carbonatite melts. The top of asthenosphere extending 350 km East-side of the ridge [*(4, 5)*, orange box] is best explained by the presence of 0.005-0.035% of carbonatite. The resistive lithosphere [*(4, 5)*, blue box] matches the conductivity of dry olivine, whereas the lithosphere below the ridge axis is characterized by a broad range of conductivities, with the highest range probably reflecting the contributions of the rising MOR-basalt. The expected depth of carbonate melting *(19, 20)* and the one of silicate melting *(11, 19)* are shown by the arrows on the right of the figure.

References and Notes:

1. Y. Xu, T. J. Shankland, B. T. Poe, *J. Geophys. Res.* **105**, 27865-27875 (2000).
2. S. Constable, *Geophys. J. Int.* **166**, 435-437 (2006).
3. A.G. Jones, *Lithos* **48**, 57-80 (1999).
4. R.L. Evans *et al.*, *Nature* **437**, 249-252 (2005).
5. K. Baba *et al.*, *J. Geophys. Res.* **111**, B02101 (2006).
6. F. Gaillard, G.I. Marziano, *J. Geophys. Res.* **110**, B06204 (2006).
7. J. A. Tyburczy, H. S. Waff, *J. Geophys. Res.* **88**, 2413–2430 (1983).
8. S-I. Karato, Water in Nominally Anhydrous Minerals, Book Series: *Reviews in Mineralogy & Geochemistry*, H. Keppler, J.R. Smyth, Eds. (MSA, 2006), vol. **62**, chap.15.
9. F. Gaillard, *Earth Planet. Sci. Lett.* **218**, 215–228, (2004).
10. A. Pommier, F. Gaillard, M. Pichavant, B. Scaillet, *J. Geophys. Res.* **113**, B05205, (2008).
11. C. Aubaud, E. H. Hauri, M. M. Hirschmann, *Geophys. Res. Lett.* **31**, L20611 (2004)
12. P. Tarits, S. Hautot, F. Perrier, *Geophys. Res. Lett.* **31**, L06612 (2004).
13. S. Demouchy, S.D. Jacobsen, F. Gaillard, C.R. Stern, *Geology* **34**, 429-432 (2006).
14. D.J. Wang, M. Mookherjee, Y.S. Xu, S-I. Karato, *Nature* **443**, 977-980 (2006).
15. T. Yoshino, T. Matsuzaki, S. Yamashita, T. Katsura, *Nature* **443**, 973-976 (2006).
16. A.E. Saal , E.H. Hauri , C.H. Langmuir, M.R. Perfit, *Nature* **419**, 451-455 (2002).
17. P. Cartigny, F. Pineau, C. Aubaud, M. Javoy, *Earth Planet. Sci. Lett.* **265**, 672-685 (2008)
18. B. Marty, I.N. Tolstikhin, *Chem. Geol.* **145**, 233-248 (1998).
19. R. Dasgupta, M. M. Hirschmann, N.D. Smith, *Geology* **35**, 135-138 (2007).
20. R. Dasgupta, M.M. Hirschmann, *Nature* **440**, 659-661 (2006).
21. D.J. Frost, C. A. McCammon, *An. Rev. Earth Planet. Sci.* 36, 389-420 (2008).
22. S.S. Shcheka, M. Wiedenbeck, D.J. Frost, H. Keppler, *Earth Planet. Sci. Lett.* **245**, 730-742 (2006).
23. W.G. Minarik, E.B. Watson, *Earth Planet. Sci. Lett.* **133**, 423-437 (1995).
24. T. Hammouda, D. Laporte, *Geology* **28**, 283–285 (2000).
25. T. Kojima, Y. Miyazaki, K. Nomura, K. Tanimoto, *J. Electrochem. Soc.* **155**, F150-F156 (2008).
26. R. J. Sweeney, *Earth Planet. Sci. Lett.* **128**, 259-270 (1994).
27. C. Simonnet, J. Phalippou, M. Malki, A. Grandjean, *Rev. Sci. Inst.* 74, 2085-2091 (2003).
28. D.P. Dobson *et al.*, *Earth Planet. Sci. Lett.* **143**, 207-215 (1996).
29. M. J. Genge, G.D. Price, A.P. Jones, *Earth Planet. Sci. Lett.* **131**, 225-238 (1995).
30. Q. Liu, R.A. Lange, *Contrib. Mineral. Petrol.* **146**, 370-381 (2003).

31. 0.35 vol.% of carbonatite melts yield mantle conductivity of 1 $S.m^{-1}$, which matches the highest value detected by geophysicists at depth of 150 km *(5)*. Such value, however, designates the conductivity in the direction parallel to the ridge axis whereas the conductivity in the perpendicular direction is 10 times lower *(5)*. We do not incorporate such anisotropic effects in our interpretation, which implies that on average 0.1 vol.% of carbonatite melts (300±200 ppmw CO_2) would be needed to explain such mantle conductivities.
32. We thank an INSU grant and the Electrovolc project, which is funded by the French national agency for research (ANR): contract JC05-42707 allocated to F.G.. We also thank two anonymous reviewers.

Table 1: Summary of experimentally defined parameter values for electrical conductivity of molten carbonates [eq.(1)]:

Compositions	**σ°** $S.m^{-1}$ (± 800)	**Ea** $J.mol^{-1}$ (± 350)	**σ at 1000°C** $S.m^{-1}$ (± 15)
$(LiNaK)_2(CO_3)_3$	6590	32,500	305
$(NaK)_2(CO_3)_2$	4177	31,427	214
$(NaKCa_{0.5})_2(CO_3)_3$	4144	32,500	192
$(NaKCa)(CO_3)_2$	2504	30,307	143
$(KCa_{0.5})_2(CO_3)_2$	3149	34,489	121
Mantle Carbonatites	3440	31,900	169

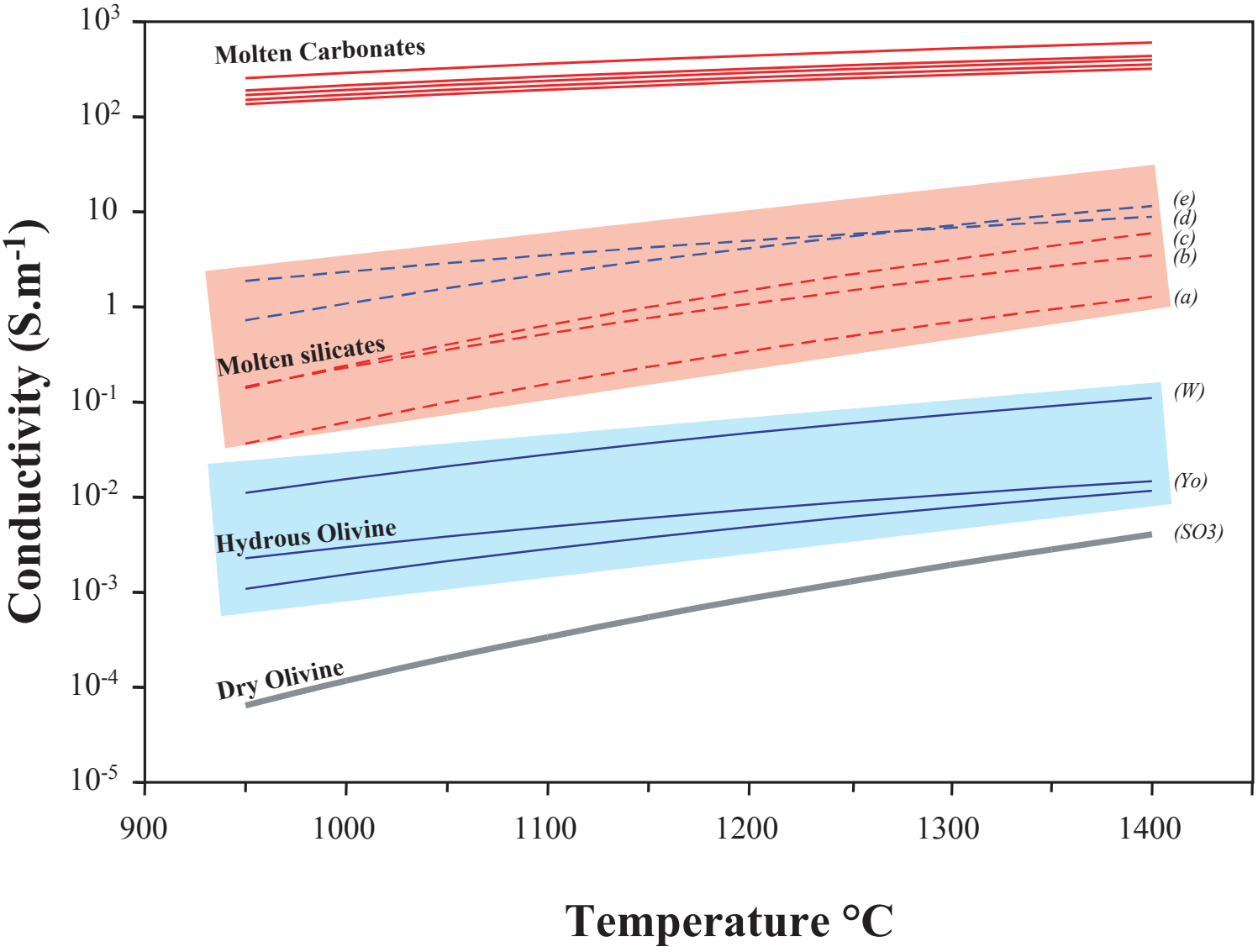
Conductivity (S.m-1)
10^3
10^2
10
1
10^-1
10^-2
10^-3
10^-4
10^-5
900
1000
1100
1200
1300
1400
Temperature °C
Molten Carbonates
Molten silicates
Hydrous Olivine
Dry Olivine
(e)
(d)
(c)
(b)
(a)
(W)
(Yo)
(SO3)

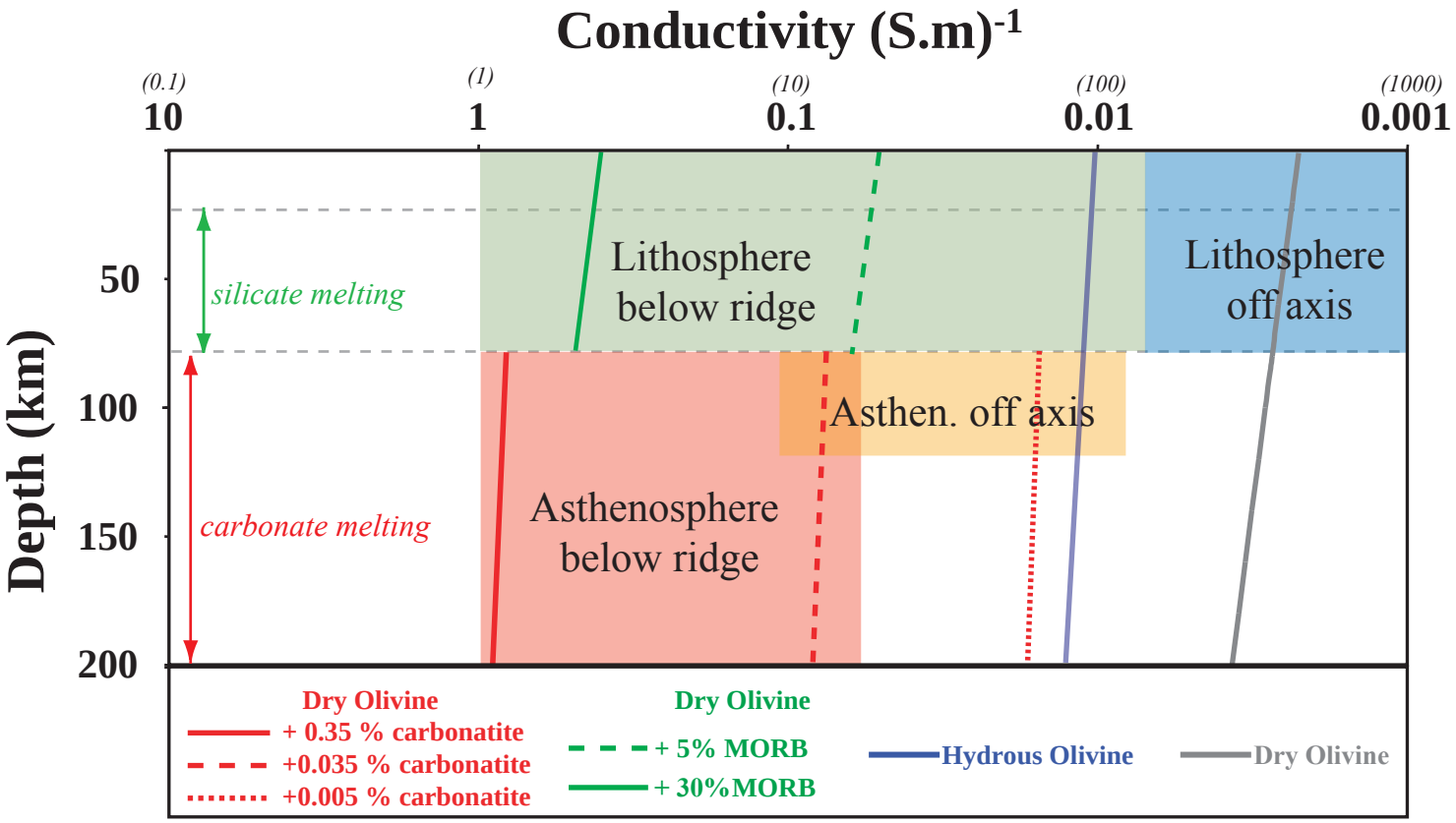
Conductivity (S.m)-1
(0.1)
10
(1)
1
(10)
0.1
(100)
0.01
(1000)
0.001
Depth (km)
50
100
150
200
silicate melting
carbonate melting
Lithosphere below ridge
Lithosphere off axis
Asthen. off axis
Asthenosphere below ridge
Dry Olivine
+ 0.35 % carbonatite
+0.035 % carbonatite
+0.005 % carbonatite
Dry Olivine
+ 5% MORB
+ 30%MORB
Hydrous Olivine
Dry Olivine